Generic two-phase coexistence, relaxation kinetics, and interface propagation in the quadratic contact process: Simulation studies

Xiaofang Guo, Da-Jiang Liu, and J. W. Evans
Ames Laboratory, U.S. DOE and Departments of Physics & Astronomy and Mathematics, Iowa State University, Ames, Iowa 50011, USA
(Received 11 December 2006; published 29 June 2007)

The quadratic contact process is formulated as an adsorption-desorption model on a two-dimensional square lattice. It involves random adsorption at empty sites and correlated desorption requiring *diagonally adjacent pairs of empty neighbors*. We assess the model behavior utilizing kinetic Monte Carlo simulations. One finds generic two-phase coexistence between a low-coverage active steady state and a completely covered or "poisoned" absorbing steady state; i.e., both states are stable over a finite range of adsorption rates or "pressures." This behavior is in marked contrast to that for equilibrium phase separation. For spatially homogeneous systems, we provide a comprehensive characterization of the kinetics of relaxation to the steady states. We analyze rapid poisoning for higher pressures above an effective spinodal point terminating a metastable active state, nucleation-mediated poisoning in the metastable region, the dynamics of poisoned droplets within the two-phase coexistence region, and behavior reminiscent of bootstrap percolation dynamics for lower pressures. For spatially inhomogeneous systems, we analyze the propagation of planar interfaces between active and absorbing states, fully characterizing an orientation dependence which underlies the generic two-phase coexistence.

DOI: 10.1103/PhysRevE.75.061129 PACS number(s): 05.70.Fh, 05.50.+q, 02.50.Ey, 05.70.Ln

I. INTRODUCTION

Stochastic spatial models for far-from-equilibrium processes incorporating irreversible steps [1] can display a richer variety of spatiotemporal behavior than traditional Hamiltonian systems where microscopic transition rates are constrained to satisfy detailed balance. One example of a feature specific to nonequilibrium systems is the occurrence of absorbing states, using the parlance of Markov processes, from which the system can never escape [1–4]. Nonetheless, more generally, the steady states of such nonequilibrium models often exhibit continuous (second-order) and discontinuous (first-order) phase transitions which appear analogous to equilibrium phase transitions in Hamiltonian systems [1–4]. Most effort towards exploring this analogy has focused on continuous nonequilibrium transitions where the concept of universality carries over from equilibrium transitions. In fact, a robust universality class for continuous transitions to nondegenerate absorbing states has been identified as that of directed percolation or Reggeon field theory [2–4].

For nonequilibrium processes, less attention has been paid to discontinuous transitions where universality does not apply [5–11]. However, one such well-known example is provided by the two-component Ziff-Gulari-Barshad (ZGB) model for a monomer-dimer surface reaction [5]. This ZGB model includes the following steps: random adsorption of monomers at single empty sites of a two-dimensional lattice ($d=2$), dissociative adsorption of dimers at empty pairs of sites, and irreversible reaction of adjacent monomer and dimer species. In this model, a discontinuous transition from an active (i.e., reactive) state to a monomer-poisoned absorbing state occurs for sufficiently high monomer adsorption rate or "partial pressure" [5]. Various phenomena related to this nonequilibrium transition have been analyzed in some detail: the steady-state coverage versus partial pressure including the pressure at the discontinuous poisoning transition [5], propagation and fluctuation behavior of interfaces between active and poisoned states [5,7,8], epidemic properties related to an active droplet embedded in the monomer-poisoned absorbing state [6,9], and nucleation of droplets of the absorbing state within the metastable active state and associated metastability phenomena [7,11]. Some features of the observed behavior are unusual for a discontinuous transitions [10] (e.g., apparent algebraic scaling of epidemic properties [6]) and likely reflect the presence of a weak line tension at the interface between active and absorbing states. We explore this latter issue elsewhere [12].

To facilitate a fundamental understanding of discontinuous nonequilibrium phase transitions, it is more convenient and natural to search for and analyze single-component models with the desired behavior (as an alternative to further analysis of the more complex two-component ZGB model). Such simpler single-component models which purportedly exhibit discontinuous transitions in low dimensions have also been developed and analyzed previously. The so-called Bidaux-Boccara-Chaté model [13] is a probabilistic cellular automaton which exhibits a discontinuous transition in $d \geqslant 2$ dimensions, but not for $d=1$ [2]. The so-called triplet-creation model [14] was developed to provide an example of a model with a discontinuous transition for $d=1$ at least for sufficiently rapid particle hopping. The issue of the existence of this discontinuous transition in this model has also been addressed in more recent studies [15]. Schloegl's second model for autocatalysis, described in more detail below, provides another example of a single-component model designed with the potential to exhibit a discontinuous transition.

There has been considerable interest in the class of Schloegl-type models associated with autocatalytic kinetics [16], where mean-field versions provide classic examples of

bifurcation behavior and synergetics [17]. Special cases of this kinetics are as follows: $X \leftrightarrow 2X$ and $X \rightarrow \emptyset$ for Schloegl's first model and $2X \leftrightarrow 3X$ and $X \rightarrow \emptyset$ for Schloegl's second model, where X denotes a particle (so, e.g., $X \rightarrow \emptyset$ represents particle annihilation). The mean-field kinetics is quadratic for the first model, suggesting a continuous transition to the vacuum state, and cubic for the second model, suggesting a discontinuous transition. It is indeed the case that various discrete realizations of the first model exhibit a continuous transition in the universality class of directed percolation. However, contrasting early reports, one careful study of a synchronous cellular-automaton type realization of the second model [18] reported a continuous transition for spatial dimension $d=1-3$. A discontinuous transition emerged only for $d \geqslant 4$. Another study of a lattice-gas model realization confirmed the existence of a continuous transition for $d=1$ [2]. Both studies actually included particle hopping which should if anything enhance a discontinuous transition given that bistability is exhibited by the mean-field version of the model. However, within the context of the current study, it should be recognized that model behavior will depend on the specific discrete realization.

In this work, we adopt a realization of Schloegl-type models on a square lattice ($d=2$) which is in the spirit of adsorption-desorption models. These models are also referred to as a "contact processes." Roughly speaking, the following adsorption-desorption prescription interchanges the role of particles and vacancies from that in the above description of Schloegl models. In the standard contact process (SCP) which mimics Schloegl's first model, particles adsorb randomly on the empty sites at fixed rate or "pressure" and desorb at a rate proportional to the number of empty nearest-neighbor (NN) sites [2–4]. Not surprisingly, this process exhibits a continuous poisoning transition to a completely covered surface (an absorbing state) which is in the directed percolation universality class. In the quadratic contact process (QCP) which mimics Schloegl's second model, again particles adsorb randomly on the empty sites at fixed rate or "pressure" and desorb at a rate proportional to the number of *diagonally adjacent pairs of empty NN sites* [1,19]. We have recently shown that this QCP exhibits a discontinuous poisoning transition between an active state with a low-coverage and a completely covered surface (again an absorbing state) [19]. These models are related to more general threshold contact processes with random adsorption where desorption is allowed (at a single rate) only if M or more adjacent sites are empty [20]. Then, the case $M=1$ is similar to the SCP, $M=2$ to the QCP (as discussed further below), and models with $M \geqslant 3$ have no active state for any $p>0$ on a square lattice. For $M=3$, particles within completely filled rectangular regions cannot desorb, so these regions spread irreversibly. For $M=4$, no particles in clusters of any shape cannot desorb, so all clusters spread irreversibly.

The traditional picture for discontinuous transitions to absorbing states is that the active and absorbing states coexist at a unique equistability pressure. Remarkably, for the QCP, coexistence of stable active and absorbing states occurs for a finite range of pressure. This means that for any pressure in this range, droplets of the absorbing state embedded in the active cannot grow indefinitely but rather die out, even though the absorbing state is stable. Likewise, droplets of the active state embedded in the absorbing state cannot grow indefinitely and instead die out. This feature leads to so-called generic two-phase coexistence (PC) or true bistability [21], which dramatically contrasts the behavior for discontinuous equilibrium transitions. For the QCP, PC can be understood in terms of an orientation dependence of the propagation of planar interfaces between active and absorbing states [19], as described in more detail in the following sections.

We should note that the prototype for such PC phenomenon is provided by Toom's synchronous north-east-center (NEC) stochastic cellular-automaton model [22–25]. In this model, individuals located on a square lattice change their votes for one of two parties guided by the majority of their current vote and those of their neighbors to their north and east. However, some biased randomness or noise is also included in the rules for voting. The overall magnitude of this noise corresponds to an effective temperature, and the bias towards one of the two parties is analogous to the application of an external magnetic field in the Ising model. PC occurs below a critical noise amplitude for sufficiently small bias. This behavior is elucidated by a heuristic analysis of the evolution of droplets of preferred party votes embedded in a state dominated by votes for the disfavored party. This analysis reveals that these preferred droplets do not grow, but rather shrink at a finite rate [23,24]. The strong asymmetry in the voting rules is believed to be responsible for PC, which also occurs in continuum analogs of the Toom model [25].

The outline of this paper is as follows. In Sec. II, we first specify our discrete stochastic lattice-gas (LG) model for the QCP on a square lattice, emphasizing a special feature of the dynamics in this model. We also describe our kinetic Monte Carlo simulation procedures. Then, we characterize the steady-state behavior for the model, specifically generic two-phase coexistence, which was observed in our previous simulation study [19]. Next, in Sec. III, we focus on simulation results for the kinetics of relaxation to the steady states of the QCP for spatially homogeneous systems. We identify an "effective" spinodal point terminating a metastable active state for pressures above the two-phase coexistence region and describe "rapid" relaxation or poisoning kinetics for pressures above this spinodal pressure. We also analyze nucleation-mediated relaxation or poisoning for pressures in the metastable region, and we characterize the dynamics of poisoned droplets within the two-phase coexistence region. In addition, for lower pressures below the two-phase coexistence region, some unusual aspects of relaxation kinetics are elucidated by making a connection to bootstrap percolation models. In Sec. IV, we analyze the propagation of interfaces with various orientations between the absorbing and active states in spatially inhomogeneous systems. As noted above, the dependence of propagation and equistability on interface orientation underlies the generic two-phase coexistence in the QCP. A summary and discussion of other models with generic two-phase coexistence, and of various generalized QCP-type models, is presented in Sec. V.

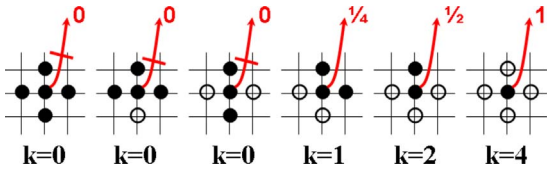

FIG. 1. (Color online) Schematic of desorption processes and rates in the QCP. Solid (open) circles denote particles (empty sites) on the square lattice. Desorption rates (k values) for the central particle are indicated above (below) the various configurations.

II. ADSORPTION-DESORPTION MODEL FOR QCP: STEADY-STATE BEHAVIOR

Our adsorption-desorption model realization of the QCP on a square lattice involves the following steps [1,19]: random adsorption of particles at empty sites at rate or "pressure" p and cooperative desorption of particles at rate $k/4$ where $k=0$, 1, 2, or 4 denotes the number of *diagonally adjacent pairs of NN empty sites*. Thus, one has $k=0$ for particles with just zero or one empty NN sites and also for two empty NN sites which are on opposite sides of the particle, $k=1$ for particles with just two diagonally adjacent empty NN sites, $k=2$ for particles with three empty NN sites, and $k=4$ for particles with all four NN sites empty, as shown in Fig. 1. Below we use $\theta=\theta(p,t)$ to denote the coverage—i.e., the fraction of filled sites—which generally evolves with time. Also $\theta_{ss}=\theta_{ss}(p)$ denotes the value of θ in the active steady state which, intuitively, one expects to exist at least for low p. In fact, the existence of such a state for sufficiently small p has been proved rigorously [20,26]. In this small-p regime, most particles are isolated with a desorption rate of unity. Consequently, evolution is approximately described by Langmuir kinetics,

$$d\theta/dt \approx p(1-\theta)-\theta \quad \text{for } p \ll 1, \quad \text{so } \theta_{ss}=p+O(p^2). \qquad (1)$$

For a more systematic expansion of θ with p, one might regard the QCP as a perturbation of a random adsorption-desorption model. Then, one could use a perturbation-theoretic analysis within a creation-annihilation operator formulation of the problem to analyze steady-state behavior [2]. For high p, one should expect that adsorption will swamp desorption, so that the system will reach a completely covered or "poisoned" absorbing state with $\theta=\theta(p)\equiv 1$.

Our kinetic Monte Carlo (KMC) simulation analysis of the behavior of this model is performed on "rectangular-shaped" $(L_x \times L_y)$-site square lattices with periodic boundary conditions. In conventional constant-p simulations, one specifies an adsorption rate p and then runs the simulation implementing adsorption and reaction with the appropriate relative rates. In this way, one determines both the dynamics and the steady-state behavior including the variation of the steady-state coverage $\theta_{ss}(p)$ with p. Alternatively, in a constant-coverage (CC) simulation algorithm [27], one specifies a target coverage θ and runs the simulation attempting to adsorb (desorb) if the actual coverage is below (above) the target θ. The fraction of adsorption attempts yields the pressure $p=p(\theta)$. The two simulation approaches should be equivalent for a sufficiently large system. In previous studies,

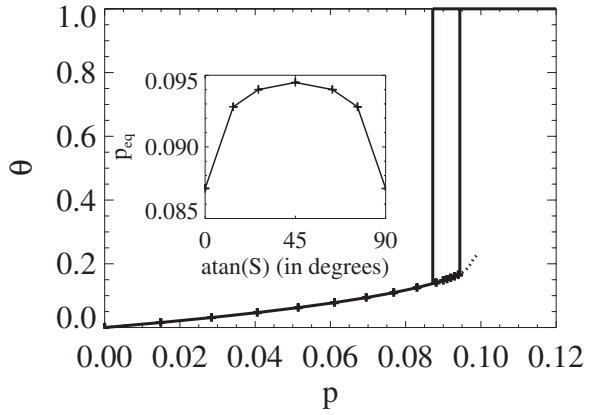

FIG. 2. Equation of state for the QCP: steady-state coverage, $\theta=\theta_{ss}$, versus p. The lower solid curve is the active steady state for which a metastable extension is indicated. The solid vertical lines denote the boundaries of the generic two-phase coexistence region. Inset: equistability pressure $p_{eq}(S)$ versus interface slope S.

the CC approach has proven particularly useful for analyzing discontinuous transitions where specifying θ anywhere in the range of the discontinuous jump of θ versus p should give the same "equistability pressure" corresponding to coexistence of the two steady states. However, for the QCP, the situation proves more complex than for conventional discontinuous transitions where one has a unique equistability pressure.

As indicated in Sec. I, simulations of the QCP demonstrate the existence of a discontinuous transition from active to absorbing states with increasing p. More specifically, starting from an empty lattice, conventional simulations reveal the evolution to a stable active state for $0 \leqslant p \leqslant p_{eq}^* \approx 0.0944$, where θ_{ss} increases monotonically with p to a maximum of $\theta_{ss}(p=p_{eq}^*) \approx 0.17$ (see Fig. 2). In this regime, simulations indicate that droplets of the absorbing state embedded in the active state never grow indefinitely; i.e., the state is stable against local perturbations (see Sec. III C for a detailed discussion). For larger p, the system eventually poisons reaching the absorbing state, as shown in Secs. III A and III B. Due to a special feature of the QCP rules described below, the absorbing state is always stable against local perturbations; i.e., an isolated droplet of the empty or active state can never grow for any $p \geqslant 0$. Thus, one might assign generic two-phase coexistence for $0 \leqslant p \leqslant p_{eq}^*$, although below we will impose a more restrictive definition.

Remarkably, CC simulations reveal that the equistability pressure at which a stationary planar interface is formed between the active and absorbing states depends on the interface orientation S [19]. We denote this pressure by $p_{eq}(S)$. These simulations were performed in a rectangular system with $L_y=SL_x$ containing an initial perfect strip of the absorbing state with slope S. The strip quickly equilibrated but remains stable, its overall slope being preserved by the periodic boundary conditions. Specifically, $p_{eq}(S)$ displays a maximum of $p_{eq}(S=1)=0.094\,43\pm0.000\,03$ (corresponding to p_{eq}^*) and decreases with increasing S to a minimum of $p_{eq}(S\to\infty)=0.0869\pm0.0005$ [19]. By symmetry, one has that $p_{eq}(S)=p_{eq}(1/S)$. Conventional simulations support these ob-

servations: for $p<p_{eq}(S)$, the active state displaces the absorbing state separated from it by a planar interface of slope S, and for $p>p_{eq}(S)$, the opposite is true. See Sec. IV for a comprehensive analysis of interface propagation.

Reformulating the above observations, for $p_{eq}(S=\infty)<p<p_{eq}(S=1)$, the active state will displace the absorbing state separated from it by a planar interface with a slope sufficiently close to unity. Also, the absorbing state will displace the active state separated by a planar interface with a slope sufficiently close to $S=\infty$. Thus, in this regime, both states are stable against certain nonlocal interfaces, in addition to being stable against local perturbations by embedded droplets. Using this more restrictive definition, we associate PC only with the regime $p_{eq}(S=\infty)<p<p_{eq}(S=1)=p_{eq}^{*}$. Certainly, we are not providing a rigorous proof of PC for this model. However, we believe that the discussion in Sec. III C provides a clear heuristic picture. Finally, we mention that for $0\leqslant p\leqslant p_{eq}(S=\infty)$, the absorbing state is not stable relative to the active state separated from it by a planar interface with any slope $0<S<\infty$.

At this point, it is appropriate to emphasize that the specific form of the desorption rules in the QCP implies certain special features for the dynamics in this model. First, it is clear that a vertical strip of the poisoned state (or even a single vertical column) can never be eroded for any $p\geqslant 0$. The same is true for horizontal strips. Particles in such strips can never have more than one empty NN site and thus have $k=0$. Consequently, analysis of the evolution of vertical strips and the determination of $p_{eq}(S=\infty)$ above are quite delicate: while a vertical strip will not expand in an infinite system for $p\leqslant p_{eq}(S=\infty)$, it will expand in a finite system due to the certainty of completion of additional filled rows of sites (which corresponds to falling into a new absorbing state). Thus, careful analysis of the size dependence of behavior is required to accurately determine $p_{eq}(S=\infty)$ [19]. Second, an isolated empty patch or an isolated patch of the active state embedded in the absorbing state can never grow outside of a rectangle inscribing that patch. Thus, eventually, the patch must be filled in for any $p>0$; i.e., the system will evolve to the absorbing state with probability of unity [1]. This feature automatically guarantees the above mentioned stability of the absorbing state against local perturbations for any $p>0$.

Finally, having introduced our adsorption-desorption version of the QCP, we mention that one motivation for consideration of such lattice-gas models is application to the modeling of catalytic reactions on single-crystal surfaces. Such reactions can exhibit discontinuous poisoning-type transitions. The ZGB model [5] was intended to describe surface science studies of CO oxidation on single-crystal catalyst surfaces. However, under typical low-pressure conditions, CO has a high surface mobility which produces a strong bistability rather than a discontinuous transition [28]. Thus, the jump in coverages or in the CO_2-production rate observed experimentally upon increasing the CO partial pressure corresponds to a spinodal point, rather than to the discontinuous transition at an equistability point. In fact, behavior with strong bistability is better captured by hybrid models directly incorporating infinite CO mobility but finite mobility for oxygen [28]. However, for high-pressure catalysis, CO surface mobility is inhibited which allows strong fluctuations and sharp interfaces to develop. In this regime, basic aspects of behavior could be qualitatively similar to that displayed by simpler ZGB- or QCP-type models with limited or zero surface mobility [29].

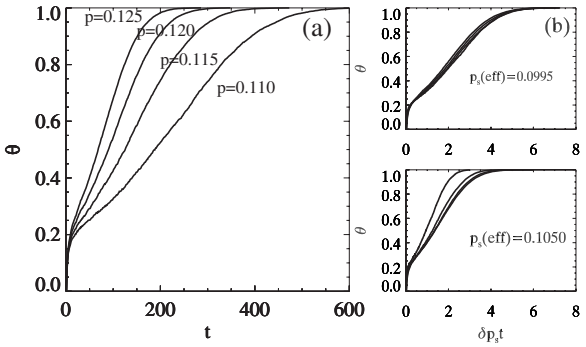

FIG. 3. (a) Rapid poisoning kinetics above the effective spinodal point p_s(eff) for a range of $p=0.110$, 0.115, 0.120, and 0.125. (b) Scaled poisoning kinetics for the above p values indicating that $p_s(\text{eff})=0.0997\pm0.0005$.

III. RELAXATION KINETICS IN THE QCP

A. "Rapid" poisoning kinetics above the metastable region

The traditional picture of discontinuous transitions holds that a state which is stable below the transition extends to a metastable state above the transition for a finite region in parameter space which is terminated by a spinodal point. Thus, for the QCP, one would expect a metastable active state to exist for some finite range of $p>p_{eq}(S=1)$. However, the precise nature and even the existence of such metastable extensions is a subtle question. For equilibrium Ising-type interacting lattice-gas models, it has now been demonstrated rigorously that there does not exist a unique analytic metastable extension of the stable state above the transition [30,31]. Consequently, the spinodal point is not uniquely defined. However, instead one can generate a C^{∞} family of metastable extensions in a rather natural and simple way by following the dynamics of the model. The latter approach is adapted for the QCP below in Sec. III B.

For the QCP (and for similar models with discontinuous transitions), one might expect that there exists some "effective" spinodal value p_s(eff) (or narrow range of p values), such that poisoning for $p>p_s$(eff) occurs much more quickly than in the metastable region for $p_{eq}(S=1)<p<p_s(\text{eff})$. Based on mean-field theories (see Ref. [32] and Appendix A), for $p>p_s$(eff), one might expect the rate of poisoning to be controlled primarily by the distance from the effective spinodal, $\delta p_s=p-p_s(\text{eff})$ at least for sufficiently small δp_s. In this case, one has that $\theta\approx\theta(\delta p_s t)$. Thus, an estimate of p_s(eff) can be made by plotting θ versus $\delta p_s t$ and achieving collapse of curves for suitable choice of p_s(eff). A similar approach was reasonably effective for the ZGB model and its extensions to include surface mobility [7]. Figure 3(a) shows the evolution of θ versus t starting from an empty lattice at

$t=0$ for a range of $p=0.110-0.125$ expected to be above p_s(eff). Indeed, good collapse of these curves plotted against the rescaled time $\delta p_s t$ is achieved choosing p_s(eff) $\approx 0.0997 \pm 0.0005$, as shown in Fig. 3(b). Similar results are achieved using a higher range of $p=0.0130-0.0145$ with a value of p_s(eff) in the range specified above yielding the best collapse.

B. Nucleation-mediated poisoning in the metastable region

To motivate our analysis of nucleation-mediated poisoning for the QCP, it is appropriate to first review the heuristic framework for nucleation in equilibrium models. The basic idea is that there exists a finite free energy barrier E_{nuc} to the nucleation of a critical droplet of the stable phase in a background of the metastable phase (where subcritical droplets shrink and supercritical droplets grow). One can show that $E_{\text{nuc}} \approx b\sigma^2/\Delta$. Here, $b>0$ is a constant, σ denotes the line tension of the interface between the coexisting states at the transition, and Δ is a measure of the (small) distance from the transition—i.e., the driving force for creation of the stable phase [31]. Then, critical droplets of the stable state are nucleated at a rate $k_{\text{nuc}} \propto \exp(-\beta E_{\text{nuc}})$, where β is the inverse temperature. Once critical droplets are formed, they grow with a velocity $v \propto \Delta$ [31] ignoring finite-curvature corrections. We consider a large system where the nucleation-mediated transition from the metastable to the stable state occurs by the spontaneous formation and growth of many supercritical droplets. The kinetics of this process is reasonably described within a continuum two-dimensional Avrami formulation [33]. In such formulations, droplets are nucleated at random locations in the plane at a fixed rate and thereafter expand at constant velocity with a fixed shape. If θ_{m} (θ_{s}) denotes the density in the metastable state (stable state), then it follows that

$$\theta(t) \approx \theta_{\text{m}} + (\theta_{\text{s}} - \theta_{\text{m}})\{1 - \exp[-a(t/\tau_{\text{char}})^3]\}, \tag{2}$$

where

$$\tau_{\text{char}} \propto v^{-2/3} k^{-1/3}.$$

Using the results above, the characteristic time for nucleation satisfies $\tau_{\text{char}} \propto \Delta^{-2/3} \exp(\lambda_{\text{nuc}}/\Delta)$ where $\lambda_{\text{nuc}} \approx \frac{1}{3} b\beta\sigma^2$. The procedure for generating a C^∞ family of metastable states (labeled by λ) is to run the dynamics starting from a suitable state near the metastable state for a time τ_{run} or the order of $\exp(\lambda/\Delta)$ where $\lambda < \lambda_{\text{nuc}}$ [30,31]. Since τ_{run} diverges exponentially as $\Delta \to 0$, it is not surprising that one obtains a C^∞ extension of the stable state. However, such extensions can vary strongly with λ and have somewhat limited physical significance. Thus, they may provide limited insight into the location of any effective spinodal point. Extensions with the most physical significance presumably correspond to choosing λ close to λ_{nuc}.

For the nonequilibrium QCP, it is reasonable to propose that the rate of nucleation of critical droplets of the absorbing state within a background for the metastable state for $p > p_{\text{eq}}(S=1)$ satisfies

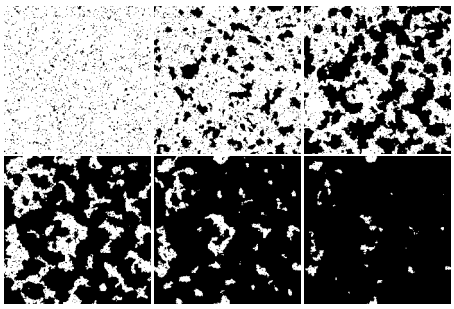

FIG. 4. Images of QCP configurations in a (1024×1024)-site system during nucleation-mediated poisoning for $p=0.098$ in the metastable region. Images correspond to unevenly spaced times but roughly equal coverage increments (time increasing from left to right, top then bottom rows, with coverages of 0.20, 0.35, 0.57, 0.76, 0.90, and 0.97).

$$k_{\text{nuc}} \propto \exp(-c_{\text{nuc}}/\delta p), \tag{3}$$

where

$$\delta p = p - p_{\text{eq}}(S=1) > 0,$$

noting that $\delta p > 0$ replaces $\Delta > 0$ above (cf. Ref. [11] which considers the ZGB model). The parameter c_{nuc} should encode information about the effective line tension between coexisting active and absorbing states in the QCP. These critical droplets will grow with a velocity $v \propto \delta p$ [7,8,28] at least if one ignores corrections due to finite curvature. Then, (2) should apply to this nonequilibrium system defining a characteristic time

$$\tau_{\text{char}} = (\delta p)^{-2/3} \exp[c_{\text{nuc}}/(3\delta p)], \tag{4}$$

and setting $\theta_{\text{s}}=1$ corresponding to the stable absorbing state. To obtain a C^∞ family of extensions of the active state (labeled by $c < c_{\text{nuc}}$), one can naturally run the QCP starting from an empty lattice for a time $\tau_{\text{run}}(c) \propto (\delta p)^{-2/3} \exp[c/(3\delta p)]$. More practically, a natural extension might be obtained by choosing τ_{run} as some fixed small fraction of τ_{char}. One such metastable extension is shown in Fig. 2.

Our focus here is on analyzing the Avrami-type nucleation-mediated poisoning kinetics in the QCP for suitably small δp and in extracting a value for the key parameter c_{nuc}. The value of $p > p_{\text{eq}}(S=1)$ (determining δp) cannot be chosen too high since one must remain within the metastable region. On the other hand, δp cannot be too small since then simulations for a finite-size system would generate only a single droplet rather than the multiple droplets assumed in our Avrami analysis [11]. The value $p=0.098$ (or $\delta p \approx 0.0036$) for a (1024×1024)-site system meets these requirements, and Fig. 4 shows the corresponding evolution during poisoning. To quantify the kinetics, Fig. 5(a) shows the evolution of θ versus t starting from an empty lattice at $t=0$ for a range of $p=0.0975-0.0990$ in the metastable region above $p_{\text{eq}}(S=1) \approx 0.0944$. Collapsing these curves by plotting against a rescaled time t/τ_{char} indicates an optimum choice of c_{nuc} in the range $c_{\text{nuc}}=0.02-0.03$, as shown in Fig.

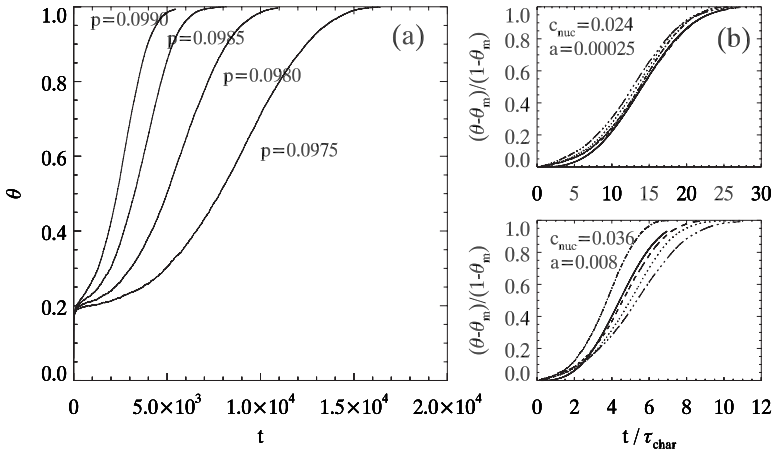

FIG. 5. (a) Nucleation-mediated poisoning kinetics in the metastable region for a range of $p=0.0975$, 0.0980, 0.0985, and 0.0990. Data are taken from simulations on a large (1024×1024)-site lattice to ensure the system is in the multidroplet regime and to reduce significant statistical fluctuations. (b) Scaled poisoning kinetics for the above p values in terms of the characteristic time τ_{char} given in the text. The best data collapse is for $c_{\text{nuc}}=0.024$. Also shown as solid curves are the Avrami kinetics (1) with best-fit values of $a=0.0002$ ($c_{\text{nuc}}=0.024$) and $a=0.008$ ($c_{\text{nuc}}=0.036$).

5(b). We also confirm that the shape of these collapsed curves is well described by the Avrami form (2).

Of course, the detailed evolution of configurations in the QCP, as shown in Fig. 4, is somewhat different than in classic continuum Avrami models. This is partly due to discrete lattice effects and partly due to fluctuations in the shapes of growing droplets. It is thus appropriate to note that discrete lattice versions of the Avrami model with deterministic droplet growth have been developed for which the kinetics is also exactly solvable and significantly for which the kinetics have essentially the same form as in the continuum model [34]. Perhaps, even more relevant is the observation that lattice versions of the Avrami model with stochastic droplet growth have also been developed. These are usually referred to as cooperative sequential adsorption (or filling) models [34,35]. Evolving configurations in these simple irreversible models do resemble those for the QCP shown in Fig. 4.

C. Dynamics of poisoned droplets in the two-phase coexistence region

Next, we further elucidate the unusual generic two-phase coexistence or true bistability exhibited by the QCP. For $p_{\text{eq}}(S=\infty)<p<p_{\text{eq}}(S=1)$, we consider the evolution of poisoned droplets of the absorbing state which are embedded in the active state. Such droplets form spontaneously, although in our study it is more convenient to embed such droplets "by hand." Since the absorbing state is stable, we must rationalize why such droplets ultimately disappear rather than grow until the (stable) absorbing state takes over the system.

To characterize such droplet dynamics, it is instructive to focus on a "worst-case scenario." Imagine that a square-shaped droplet is formed or created with sides orientated with the principal lattice directions (i.e., with slopes $S=0$ and $S=\infty$). Then, since $p>p_{\text{eq}}(S=\infty)$, the sides of this droplet should initially tend to grow outwards with finite velocity. Assuming that growth at the corners of this droplet is inhibited, one expects a tendency towards the development of a roughly octagonal shaped droplet. Then, since $p<p_{\text{eq}}(S=1)$, the facets with slope $S=\pm1$ at the corners will tend to shrink and the sides with slopes $S=0$ or ∞ will grow out, yielding a diamond-shaped droplet. Thereafter, this diamond-shaped droplet will naturally shrink. From standard simulations, we can readily explore the progression of droplet shapes for various p. Such analyses reveal that the simple progression in geometric shapes mentioned above is somewhat concealed due to large fluctuations. Figure 6 shows simulations with an initial (128×128)-site droplet and with $p=0.0940$. Even with this large size and "high" p close to $p_{\text{eq}}(S=1)$, fluctuations in droplet shape are significant and shrinkage of clusters starting at the corners is perhaps more evident than growth of the $S=0$ and $S=\infty$ sides. However, analysis of the total coverage of the system during this simulation (not shown) does reveal an initial increase corresponding to the regime of net growth from a square- to diamond-shaped droplet. Then, a fairly sudden transition occurs to a regime of nonlinear decrease of the total coverage consistent with the picture of a diamond-shaped cluster shrinking with constant velocity.

Of course the above analysis of droplet evolution is heuristic rather than rigorous and the understanding of behavior at droplet corners is limited. However, as droplets become larger, a simple deterministic geometric picture of evolution becomes more applicable where behavior is controlled by the orientation dependence of the propagation of planar interfaces. In contrast, for smaller clusters, simple geometric evolution is largely concealed by fluctuations.

D. Relaxation kinetics for $p=0$ or $p=0+$: Bootstrap percolation

Relaxation behavior for p below the two-phase coexistence regime is strongly impacted by the special feature of the

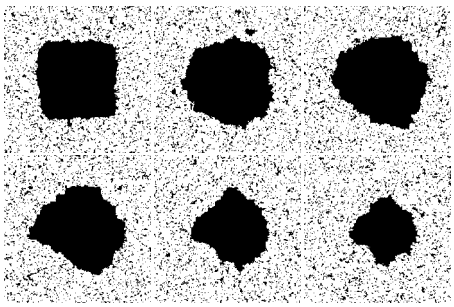

FIG. 6. Dynamics of a large initially square poisoned droplet in the two-phase coexistence region for $p=0.0940$. The system size is 256×256 sites, and the initial droplet size is 128×128 sites. Images are shown for equal time increments of ~4000 time units (time increasing from left to right, top then bottom rows).

QCP which makes the absorbing state stable against localized perturbations (i.e., an isolated active or empty droplet embedded in the absorbing state can never survive). In general, to systematically analyze relaxation kinetics in models with unstable or metastable absorbing states, typically one might start with a state corresponding to a lattice partially filled by a random distribution of particles with initial coverage θ_i. Then, for low initial vacancy concentrations, $\theta_v = 1-\theta_i \ll 1$, the system is initially close to the absorbing state and one can follow evolution to the active state [7].

However, there is some deviation from this simple scenario for the QCP. First, consider the simplest case for $p=0$ where particles with $k>0$ irreversibly desorb in the absence of adsorption. For a strictly finite $(L_x \times L_x)$-site system (i.e., $L_x=L_y=L$, say), one might expect the following scenario described in terms of "small" critical value for $\theta_v=\theta_v^*(L)$. For $\theta_v<\theta_v^*$, empty square or rectangular patches will be formed and grow around any clusters of vacant sites. However, typically the system will eventually "freeze" into a distribution of small isolated nonoverlapping empty rectangles. (This distribution will include vacant squares and single vacant sites.) In this case, the system would never reach the active state for $p=0$ which corresponds to an empty lattice. For $\theta_v>\theta_v^*$, these growing vacant rectangular patches can link sufficiently to percolate and this leads to the ultimate removal of all particles from the lattice.

More generally, for infinitesimal nonzero pressure $p=0+$, it then follows that this system of size L would typically reach the active state only for $\theta_i<\theta_i^*(L)\equiv 1-\theta_v^*(L)$ and would eventually reach the absorbing state for $\theta_i>\theta_i^*(L) \equiv 1-\theta_v^*(L)$. Indeed, simulations indicate that there does exist such a critical value for the initial vacancy coverage, although behavior as $L=L_x\to\infty$ is more subtle as we describe below.

A detailed characterization of the above critical behavior follows from recognizing that the dynamics of the $p=0$ QCP model maps onto that of a specific bootstrap percolation (BP) model. In the standard BP model on a square lattice, one culls particles which have a two or more neighboring empty sites [36,37]. This standard BP model is isomorphic to that of so-called $2n$ diffusion percolation ($2n$ DP) on a square lattice where one adds particles at empty sites if any two or more neighboring sites are occupied [36]. The QCP dynamics for $p=0$ is actually isomorphic to a variant of $2n$ DP denoted by $s2n$ DP which requires at least two of the occupied neighbors of the empty site be diagonal neighbors [36].

We translate the key result for these types of BP or DP models into the language used in the current paper where one starts with a "small" random distribution of vacancies of density θ_v on an otherwise occupied lattice and progressively removes particles according to the prescribed QCP rules. Then, there exists a constant γ such that the critical value $\theta_v^*=\theta_v^*(L)$ of the vacancy density satisfies $\theta_v^*\approx\gamma/\ln(L)$, as $L\to\infty$. Thus, one has $\theta_v^*\to 0$ and $\theta_i^*\to 1$, as $L\to\infty$; i.e., an infinite system will always reach the active state no matter how close is the initial coverage, $\theta_i<1$, to unity. A more common presentation of this result is that for a fixed initial θ_v, there exists a critical linear system size $L=L^*(\theta_v) \sim \exp[\gamma/\theta_v]$, such that when $L\ll L^*$, typically frozen distributions of isolated empty rectangular patches result. However, for L considerably in excess of L^*, the lattice will typically completely empty. The above relationships have been demonstrated rigorously for the standard BP or $2n$ DP model [38,39] and are supported by numerical simulations for several variants (including $s2n$ DP). The dynamics of interest for small θ_v relies on rare bottleneck events—i.e., the linkage of large clusters of vacant sites, which has also been described as "capture of a critical droplet" [38].

A key conclusion from the above results is that there are very strong finite-size effects on the dynamics as reflected by the exponential increase of L^* with the inverse of θ_v. Simulation results indicate that $\gamma\approx 0.25$ for standard BP considering sizes up to $L\approx 2\times 10^4$ (although this γ value is far from the true asymptotic value [39]) and $\gamma\approx 0.47$ for $s2n$ DP or the $p=0$ QCP considering sizes up to $L\approx 800$ [37]. The larger value of γ in the latter case should be expected since desorption is more difficult for the $p=0$ QCP than for standard BP. Thus, for a given size L, a larger value of $\theta_v^* \sim \gamma/\ln(L)$ is required for percolative removal of all particles in the $p=0$ QCP compared to standard BP. Equivalently, for a given θ_v, a larger size $L^*(\theta_v)\sim\exp(\gamma/\theta_v)$ is required for such percolation in the $p=0$ QCP.

E. Relaxation kinetics for lower p: Simulation results

Next, we turn to the issue of characterizing the relaxation kinetics in the QCP for general lower (but nonzero) p starting with a random distribution of vacancies of coverage θ_v. Here, we select a finite system size—e.g., $L=256$ or 512. Then, in our standard analysis for each fixed $p>0$, we run simulations for various θ_v to determine the critical value $\theta_v^*(p,L)$ which separates evolution to a poisoned state (for $\theta_v<\theta_v^*$) and to the active state for $(\theta_v>\theta_v^*)$. In the former case, the system evolves to produce an array of separated active droplets which can be inscribed within a distribution of nonoverlapping isolated rectangles. Once such a state is achieved, it is clear that the system must eventually evolve to an absorbing state just as for $p=0+$. For the latter case, the active droplets link sufficiently to percolate, leading to evolution to the active state. Strictly speaking, for θ_v sufficiently close to θ_v^*, there can be a significant probability for the system to reach either absorbing or active state. Thus, more precisely, we should state that the system reaches the poisoned state with probability above (below) 0.5 for $\theta_v<\theta_v^*$ $(\theta_v>\theta_v^*)$. From a series of such analyses for various p, we can map out the dependence of $\theta_v^*(p,L)$ versus p. See the inset to Fig. 7(b) which actually plots a closely related quantity (see below).

The above analysis strictly applies only for $p<p_{eq}(S=1)$. However, with some ambiguity, one can extend the analysis into the metastable region at least for p slightly above $p_{eq}(S=1)$. Here, the critical coverage $\theta_v=\theta_v^*(p,L)$ separates evolution to the absorbing state and to the metastable state as shown in Fig. 7(a).

Choosing $\theta_v=\theta_v^*(p,L)$ for large L, one finds that after some transient period, the coverage evolves from the initial value of $\theta_i^*(p,L)=1-\theta_v^*(p,L)$ to a final value of $\theta_f^*(p,L)$ which is quasistationary for thousands of time units and is

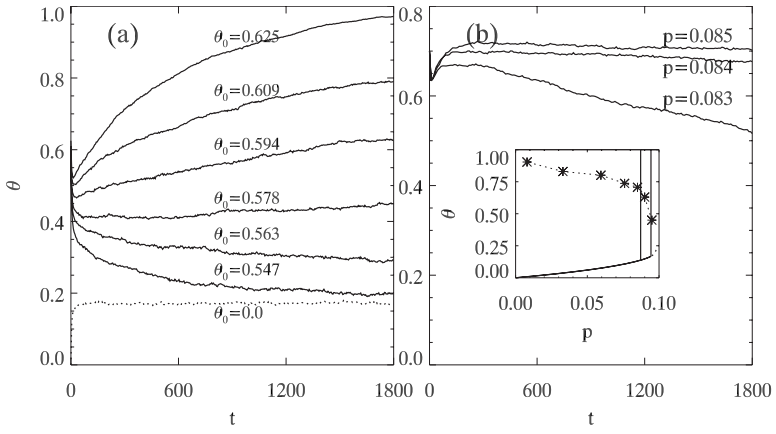

FIG. 7. (a) Relaxation kinetics for fixed $p=0.0950$ and $L=256$ in the metastable region just above the two-phase coexistence region and for varying the initial coverage $\theta_0=\theta_i$ (shown). The critical initial coverage separating evolution directly to the absorbing state and to the metastable state is $\theta_i^*(p=0.0950,L=256)\approx 0.57$ for which $\theta_f^*(p=0.0950,L=256)\approx 0.4$ Shown for comparison as a dotted line is evolution to the metastable state for $\theta_i=0$. (b) Relaxation kinetics for fixed initial coverage, $\theta_i=0.7$, varying p (shown). Inset: $\theta_f^*(p,L)$ versus p (shown as $*$ symbols) for $L=256$.

typically somewhat different from $\theta_i^*(p,L)$. For example, Fig. 7(a) shows that $\theta_i^*\approx 0.57$ versus $\theta_f^*\approx 0.4$ when $p=0.0950$ and $L=256$. We naturally map out $\theta_f^*(p,L)$ versus p, which is actually the quantity shown in the inset to Fig. 7. We regard this dependence as more fundamental than that of $\theta_i^*(p,L)$ versus p, which should depend more strongly on the specific choice of the random initial conditions. The form of the θ_f^* versus p curve is somewhat reminiscent of the variation of the unstable steady-state coverage with p in mean-field-type treatments of the QCP (see Ref. [32] and Appendix A). However, we shall see below that this behavior is not associated with an unstable steady state.

It should be emphasized that the form of $\theta_f^*(p,L)$ versus p shown in Fig. 7 exhibits significant finite-size effects. This is most obvious for $p=0+$ where $\theta_f^*(0+,L)\sim 1-\gamma/\ln(L)\to 1$, as $L\to\infty$. For moderate p, no significant finite-size effects are evident from our simulations (and this is consistent with the picture below for evolution with a quasi-steady-state coverage). However, it is difficult to rule out finite-size effects since they are weak and subtle. Nonetheless, one can say that as $L\to\infty$, at least the portion of the $\theta_f^*(p,L)$ versus p curve near $p=0$ will rise to go smoothly through $\theta_f^*(p=0,L=\infty)=1$. We assume without proof that $\theta_f^*(p>0,L=\infty)<1$.

We also note that the variation of $\theta_f^*(p,L)$ with p can be determined by an alternative analysis where simulations are performed in an $(L\times L)$-site system where one fixes $\theta_v>\theta_v^*(L)$—i.e., $\theta_i<1-\theta_v^*(L)$—and explores evolution for various p. There exists a critical pressure $p^*(\theta_v,L)$ such that for $p<p^*(\theta_v,L)$, the system will evolve to the active state and for $p>p^*(\theta_v,L)$ the system will become poisoned (since evolution produces an array of active droplets which can be inscribed within a distribution of nonoverlapping isolated rectangles) as shown in Fig. 7(b). When $p=p^*(\theta_v,L)$, after a transient period, the coverage evolves from its initial value $\theta_i=1-\theta_v$ of to a final quasistationary value of θ_f^*. Plotting this θ_f^* versus θ_i recovers the curve shown in the inset to Fig. 7.

Finally, we characterize in more detail the evolution of states with quasistationary coverage $\theta=\theta_f^*$ observed for pressure p upon choosing an initial $\theta_v=\theta_v^*(p,L)$. As noted above, such behavior is reminiscent of unstable steady states in mean-field models. In fact, robust unstable steady states can exist in lattice-gas models in the hydrodynamic limit of rapid hopping of some species [28]. However, such states are not expected for models with finite mobility. Indeed, monitoring the evolution of the system from the initial random distribution of vacancies (or filled sites) as shown in Fig. 8 reveals a complex and persistent coarsening process. Just as for BP slightly above the percolation threshold one finds slow coalescence of overlapping rectangular clusters of the active state to form progressively larger inscribing rectangular clusters. This coarsening process (which tends to reduce the coverage) is exactly counterbalanced by the filling and disappearance of isolated clusters of the active state (which tends to increase the coverage).

IV. PROPAGATION OF INTERFACES SEPARATING ACTIVE AND ABSORBING STATES

A. Analysis for a vertical interface with slope $S=\infty$

Analysis of the propagation vertical interfaces in the QCP, and thus determination of $p_{eq}(S=\infty)$, is delicate for reasons outlined below. For a finite $(L_x\times L_y)$-site system with periodic boundary conditions which includes a vertical filled strip of length L_y, particles within completely filled columns of the strip can never desorb. Consequently, the strip (and in particular its core) can never shrink. Consider the partially completed columns adjacent to the completed columns of the strip. Completion of each such column corresponds to falling into a new absorbing state. Consequently, this event must

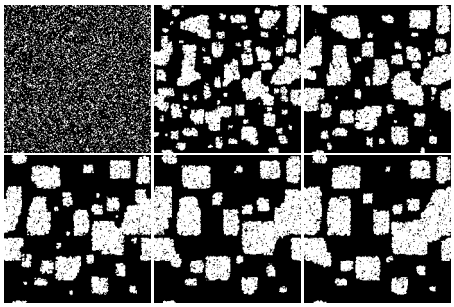

FIG. 8. Images of QCP configurations for a (256×256)-site system during the coarsening process choosing $\theta_v=\theta_v^*(p,L=256)=0.3$ (so $\theta_i=0.7$) for $p=0.084$. These parameters correspond to the central curve in Fig. 7(b). Images are shown for equal time increments of ~400 time units (time increasing from left to right, top then bottom rows).

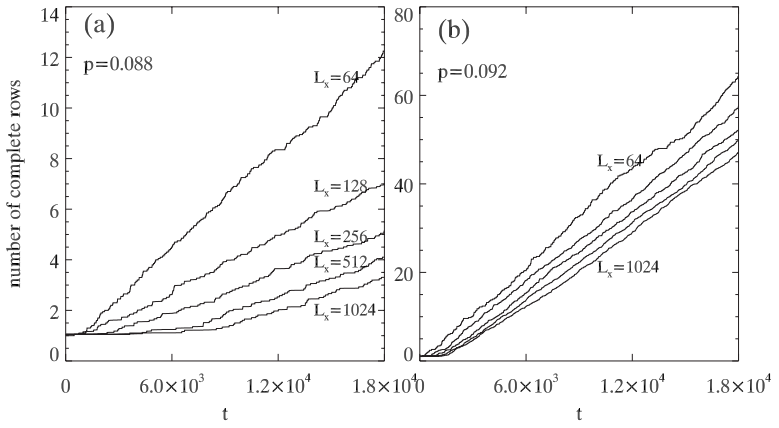

FIG. 9. Number of completed columns versus time for vertical interfaces of various lengths, $L_y=64$, 128, 256, 512, 1024 (shown). Results are presented for (a) $p=0.088$ and (b) $p=0.092$.

eventually occur with probability unity in conventional simulations (for any $p>0$) in a finite system. It must also occur in CC simulations provided there are sufficient particles in the system to allow column completion. In this sense, either conventional or CC simulations in finite systems are potentially "corrupted." This is why our previous CC simulations provided a careful analysis of finite-size effects [19]. The potential problem is that this "artificial" finite-size propagation can lead to an underestimate of $p_{eq}(S=\infty)$ if the latter is determined by the absence of any expansion of the absorbing state. We are thus motivated to systematically explore finite-size effects in standard simulations for the propagation of vertical interfaces.

One strategy to systematically assess finite-size effects is to perform simulations for a sequence of system sizes with $L_y=2^n L_x$ for increasing n containing a vertical interface of length L_y. The tendency for finite-size corruption corresponding to "artificial" column completion should decrease as $n\to\infty$. To explore this phenomenon, we show in Fig. 9 the dependence on L_y of the number of completed columns as a function of time starting with a single complete vertical column. For a lower pressure of $p=0.088$, columns are artificially completed for small L_y, but this rate of column completion appears to vanish as $L_y\to\infty$, consistent with the choice of $p\approx p_{eq}(S=\infty)\approx 0.087$. For a higher pressure $p=0.092$ satisfying $p_{eq}(S=\infty)<p<p_{eq}(S=1)$, columns are completed artificially quickly for small L_y. The rate of completion does decrease for increasing L_y, but now saturates at a finite value for $L_y\to\infty$. This is consistent with the choice $p>p_{eq}(S=\infty)$.

Finally, it is instructive to analyze the nonzero propagation velocity of a vertical interface, $V(S=\infty,p)<0$ versus $p>p_{eq}(S=\infty)$ for a large system (where finite-size corruption is negligible). Results from our standard constant-p simulation are shown in Fig. 10.

B. Analysis for interfaces with slopes $1\leqslant S<\infty$

It is appropriate to present a comprehensive analysis of the dynamics of interfaces separating active and absorbing states with various prescribed slopes S. This behavior can be obtained from standard constant-p simulations. Again, the orientation dependence of propagation underlies the generic two-phase coexistence or true bistability of the QCP. Here, we consider systems with $L_y=SL_x$ and with periodic boundary conditions starting from an initial filled strip of slope S. After a possible initial transient, the total number of filled sites in the system changes linearly in time. By monitoring this change and accounting for the different local coverages of the absorbing state, $\theta=1$, and the active state, $\theta=\theta_{ss}(p)$, as described above, one can readily extract the propagation velocity $V(S,p)$ as a function of p.

Results for $V(S,p)$ versus p with $S=1$, 2, and 4 are shown in Fig. 10 for a broad range of $p\geqslant 0$. For $0\leqslant p\leqslant p_{eq}(S)$, the active state is more stable than the absorbing state and displaces the latter (for $0<S<\infty$). We assign $V(S,p)>0$ in this case. Since $V(S,p)=0$ when $p=p_{eq}(S)$, this feature allows an independent check on the results for equistability pressures from CC simulations. Estimates of $p_{eq}(S)$ from this analysis are consistent with those presented in Sec. II. As p increases above $p_{eq}(S)$, the absorbing state becomes more stable and displaces the active state, so $V(S,p)<0$. Interface configurations corresponding to the equistability pressure are shown in Fig. 11 for various slopes S. These were obtained from CC simulations.

Some more detailed discussion is appropriate for the regime where $p>p_{eq}(S)$ and $V(S,p)<0$ as the associated in-

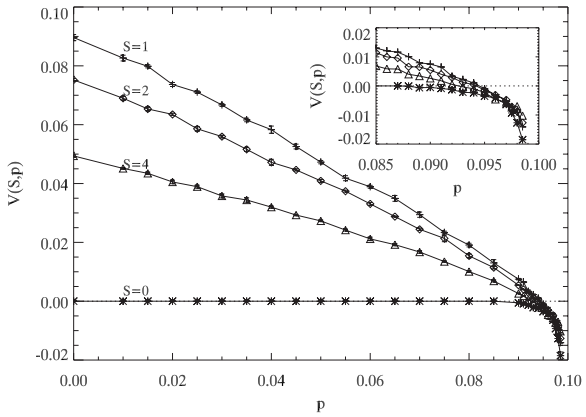

FIG. 10. Interface propagation velocity $V(S,p)$ versus p, in the QCP for broad range of p. Behavior is shown for interface slopes $S=1$, 2, 4, and ∞ (or 0). Inset: behavior near the equistability pressures and approaching the effective spinodal point. Note that $V(S=\infty,p)\equiv 0$ for $p<p_{eq}(S=\infty)\approx 0.869$ and that $V(S=\infty,p)<0$, only for $p>p_{eq}(S=\infty)$.

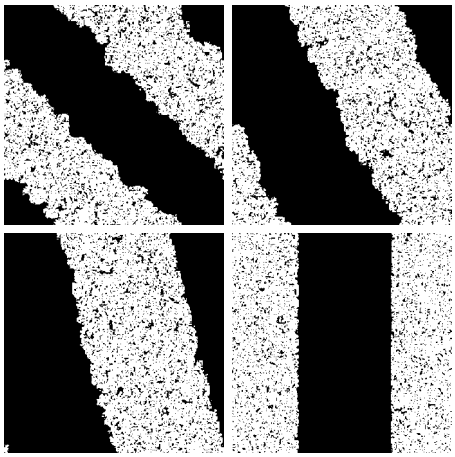

FIG. 11. Configurations of equistable interfaces between the active and absorbing states in the QCP for various interface slopes $S=1$ (top left), 2 (top right), 4 (bottom left), and ∞ (bottom right). Images sizes are 256×256 sites.

terface propagation may not be well defined. First, consider the case $S=1$ where the active state is only metastable for $p>p_{eq}(S=1)$, and so interface propagation is transient; i.e., propagation only persists until spontaneous nucleation-mediated decay of the active state. Just as for the active-state coverage, $\theta_{ss}(p)$ versus p, one does not expect there to exist a unique analytic extension of $V(S=1,p)$ versus p into the metastable region $p>p_{eq}(S=1)$. However, presumably there does exist a C^{∞} family of extensions obtained by simulation of transient front propagation for times on the order of $\tau_{run}(c)$ given in Sec. III A with and $c<c_{nuc}$. Second, consider the case $S>1$ where there is a finite range of pressure, $p_{eq}(S>1)<p<p_{eq}(S=1)$, where propagation of the absorbing state into the active state is persistent since the active state is stable against nucleation. In this regime, propagation and the associated velocity $V(S,p)<0$ are well defined. Again, a unique analytic extension will not exist for $p>p_{eq}(S=1)$.

An expanded view of the behavior of $V(S,p)$ versus p in this regime of $p\approx p_{eq}(S)$ is shown in the inset to Fig. 10. It appears that there is a confluence of the curves for different S at some p value above $p_{eq}(S=1)$. Examination of interface propagation in mean-field treatments of the QCP extended to treat spatially nonuniform systems also indicates a tendency for such velocity curves to merge quite close together at a spinodal point [32]. (This spinodal point is well defined in mean-field treatments.) Thus, Fig. 9 indicates an effective spinodal point for the active metastable state in the QCP somewhat above $p=0.098$, consistent with the analysis in Sec. III A.

C. Irreversible shrinkage of the absorbing state for $p=0$

Although not central to the analysis of generic two-phase coexistence, for a complete analysis of interface propagation in the QCP, we consider in more detail the special case when $p=0$. Here, surprisingly, we are able to present exact results for the nontrivial propagation behavior. For $0<S<\infty$, this case corresponds to irreversible shrinkage of a strip of the

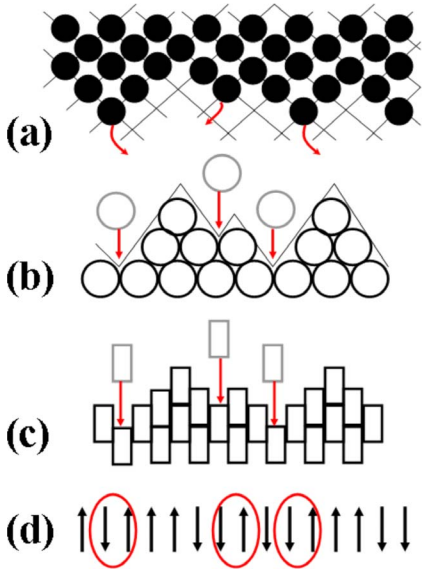

FIG. 12. (Color online) Schematic demonstrating the equivalence of (a) irreversible erosion of the absorbing state in the QCP with $p=0$, (b) interface growth in the $(1+1)$-dimensional bridge site, (c) interface growth in the single-step deposition models, and (d) evolution in a fully asymmetric spin exchange model. We indicate the active sites for erosion by desorption in the QCP (a) and for deposition in models (b) and (c). The active sites for spin exchange are circled in (d). The thin diagonal lines in (b) guide the eye in identifying local peaks and valleys of the growing interface.

absorbing state. The exact analysis is perhaps most readily achieved by recognizing that the dynamics of shrinkage the interface of the absorbing state in the $p=0$ QCP model maps exactly onto the dynamics of irreversible growth of an interface in the $(1+1)$-dimensional bridge-site deposition model [40] or, equivalently, onto the single-step deposition model [40–42]. Both these models involve random deposition at specific allowed sites. The dynamics in these models is in turn equivalent to that of a fully asymmetric spin exchange model (i.e., an up spin can exchange with a neighboring down spin only on the left, say), where spin up (down) corresponds to a step up (down) in the single-step model. Figure 12 shows an interface with mean slope $S=1$ in the QCP drawn aligned horizontally and corresponding to a flat interface in the single-step model with mean slope σ of zero. This in turn corresponds to the spin exchange model in the case of equal populations of up and down spins—i.e., with zero net magnetization (also denoted by σ). More generally, the equivalence of these models extends to interfaces and surfaces with more general orientations. Specifically, an interface with mean slope $S=(1+\sigma)/(1-\sigma)>1$ in the QCP corresponds to a surface with mean slope $0<\sigma=(S-1)/(S+1)<1$ in the single-step deposition models and vice versa (as the natural axes differ by 45°).

In the exact analysis, one considers systems with a finite width of interface (specifically, a finite width in the horizontal direction in Fig. 12 corresponding to $S=1$ or $\sigma=0$) where regular or skewed periodic boundary conditions preserve the mean slope. Then, in the reference frame moving with the interface or growing surface, there are a finite number of

possible configurations. A simple but critical observation for the deposition models is that each configuration has the same number of local valleys and peaks [41]. Thus, for the prescribed deposition dynamics, each configuration can be destroyed or created in the same number of ways. Destruction occurs by deposition which can occur only at a local valley, and creation occurs starting from a configuration which differs only by removal of a particle at one peak to create a local valley (and by deposition at that valley). This observation implies that in the steady state, all allowed configurations have the same weight [40–42]. Given this information, one can immediately calculate the steady-state values of various quantities of interest such as the density of local valleys which determines the propagation velocity. Then, one can extract values of these quantities in the limit of infinite system width (which is of primary interest).

The central result from this analysis for the single-step deposition model on an infinite surface with a deposition rate of unity is that the film growth velocity in the direction orthogonal to $\sigma=0$ satisfies $V_{\perp}(\sigma)=\frac{1}{2}(1-\sigma^2)$ for orientations $0\leqslant\sigma\leqslant 1$ [40,42]. Thus, the growth velocity normal to the mean orientation of the film surface satisfies $V(\sigma)=V_{\perp}(\sigma)/(1+\sigma^2)^{1/2}$. Translating the result into the language of the QCP for $p=0$, one must note that all particles desorbing from the eroding interface have exactly two empty NN sites, so $k=1$ and the desorption rate is $\frac{1}{4}$. Also, inspection of Fig. 12 indicates that distances must be rescaled by a factor of $1/\sqrt{2}$. Thus, it follows that infinite interfaces in the $p=0$ QCP has a propagation velocity

$$V(S\geqslant 1,p=0)=V(\sigma)/(4\sqrt{2})=\tfrac{1}{4}S(S+1)^{-1}(S^2+1)^{-1/2} \sim 1/(4S) \quad \text{as } S\to\infty. \tag{5}$$

In particular, we note that $V(S=1,p=0)=1/(8\sqrt{2})\approx 0.0884$, $V(S=2,p=0)=1/(6\sqrt{5})\approx 0.0745$, and $V(S=4,p=0)=1/(5\sqrt{17})\approx 0.0485$, consistent with simulation results. As an aside, we mention that the above exact analysis also determines finite-size corrections to the result (5).

V. SUMMARY AND DISCUSSION

Our realization of the quadratic contact process as an adsoption-desorption model on a square lattice displays generic two-phase coexistence or true bistability between an active state and an absorbing state for a range of adsorption rates of pressures. This feature derives from the dependence on interface orientation of the equistability pressure for these two states. This behavior of the QCP is in marked contrast to that for discontinuous transitions in equilibrium systems where equistability occurs at a single pressure.

Indeed, it is natural to compare behavior of the QCP with the equilibrium states of a reversible adsorption-desorption model on a square lattice with random adsorption at rate p and correlated desorption at rate $\exp[n\beta\phi]$. Here, $\beta=1/(kT)$ denotes the inverse temperature, n denotes the number of occupied NN sites, and $\phi<0$ denotes a NN attractive adspecies interaction. The equilibrium properties of this reversible adsorption-desorption model correspond to the 2D Ising model. For low pressures, the steady-state coverage satisfies $\theta_{ss}(p)=p+O(p^2)$, just as in the QCP. Below a critical temperature, $T_c=0.57\phi/k$, increasing p reveals a unique equistability pressure p_{eq}, where $\theta_{ss}(p)$ undergoes a discontinuous jump corresponding to a transition from a dilute to a dense two-dimensional phase with $\theta_{ss}(p)$ closer to unity. The discontinuous transition disappears as T approaches T_c.

From a broader perspective, generic two-phase coexistence can never occur in conventional equilibrium models such as the Ising model. This is readily understood since coexistence requires equality of the chemical potentials for the coexisting phases, and this occurs only for a single pressure. One perspective on PC in nonequilibrium models in d spatial dimensions is that the stationary distribution of histories in these models can be regarded as a constituting "generalized Ising models" in $d+1$ dimensions [23]. For these higher-dimensional systems, the free energy can be identically zero in a finite region of parameter space.

As noted in Sec. I, perhaps the prototype of generic two-phase coexistence or true bistability is provided by Toom's NEC stochastic cellular-automaton model [22]. The origin of PC in this model derives from the strong broken symmetry of the dynamic voting rules. This results in an obvious strong anisotropy in interface propagation. The dynamic adsorption-desorption rules of the QCP do not incorporate broken symmetry, and the anisotropy in interface propagation underlying PC is more subtle. One could speculate that PC in the QCP is related to the presence of an absorbing state, an intrinsically nonequilibrium feature absent in Toom's model. However, this is not the case, as shown in our discussion in Appendix B of generalizations of the QCP [19]. We should emphasize that PC has been observed in a variety of other nonequilibrium models. One such class models pertains to interface motion in the presence of pinning sites, where both pinned and propagating states exist [21]. Bistability derives from the feature that a greater driving force is required to depin an interface rather than to just maintain motion. Another class of examples derives from nonequilibrium adsorption-desorption models with enhanced binding at the substrate [43]. Under suitable conditions, PC exists between a nonwetting phase (corresponding to the film surface pinned to the substrate) and a growing phase. Although not described in Ref. [43], one can relate PC in this model to anisotropy in propagation of the growing phase. Another class of stochastic cellular-automaton models has been applied to explore generic stability of temporally periodic states (against the expected desynchronization of spatially separated regions) [44]. Again analysis of the evolution (and shrinkage) of temporally out-of-phase droplets is instructive. Currently, we are exploring the hypothesis that PC is a very general phenomenon in nonequilibrium adsorption-desorption or reaction models with discontinuous transitions, but that it is typically difficult discern due to a combination of weak orientation dependence of interface propagation and due to weak metastability.

In all of the above analyses, consideration of the evolution (and shrinkage) of droplets of one phase embedded in another is invaluable in understanding the origin of PC. Of course, the concept of critical droplets has long proved a valuable tool for characterizing metastability and nucleation-mediated kinetics in classic equilibrium models [45]. Here,

the same framework is shown to extend to the consideration of nucleation-mediated kinetics in the metastable regime just outside the two-phase coexistence regime in the nonequilibrium QCP model. We also note that this approach has been applied previously for ZGB-type models [7,11].

Finally, it is natural to consider several modifications or generalizations of the QCP: (i) introduction of an additional random desorption pathway which removes the absorbing state but preserves PC, (ii) introduction of hopping at rate h which allows connection with the mean-field QCP in the limit as $h \to \infty$, (iii) consideration of the QCP on different two-dimensional lattices which can change the nature of the phase transition to the adsorbing state, and (iv) "relaxing" the constraint on desorption in the QCP so that all particles with two or more empty neighbors can desorb (i.e., the $M=2$ threshold contact process). See Appendices A and B for further discussion.

ACKNOWLEDGMENTS

Work at the Ames Laboratory was supported by the U.S. Department of Energy (Basic Energy Sciences, Division of Chemical Sciences) under Contract No. DE-AC02-07CH11358. X.G. was also partly supported for this work by NSF Grant No. CHE-0414768.

APPENDIX A: MEAN-FIELD QCP IN THE LIMIT OF RAPID STIRRING

The QCP is naturally generalized to allow hopping of particles to NN empty sites at rate h. Introducing any degree of hopping removes the special feature of standard QCP rules which prohibits growth of isolated empty droplets embedded in the absorbing phase and which prohibits the shrinkage of vertical strip of the absorbing state (as noted in Ref. [1]).

Here, we focus on behavior in the $h \to \infty$ rapid-stirring hydrodynamic limit. We note that for this single-component model with the conventional prescription of hopping to NN empty sites, one will recover a simple description of chemical diffusion with constant diffusion coefficient $D=h$ (where spatial units are in lattice constants) [46]. In contrast, for multicomponent models, typically chemical diffusion is nontrivial in the hydrodynamic limit (even in the absence of interparticle interactions beyond site exclusion) [28]. Below, the coverage $\theta=\theta(\underline{x},t)$ at site $\underline{x}=(i,j)$ regarded as a continuous variable, and its evolution for spatially nonuniform systems is described exactly by the mean-field reaction-diffusion equation [1]

$$\partial/\partial t\,\theta = f(\theta) + D\partial^2/\partial \underline{x}^2\,\theta, \tag{A1}$$

where

$$f(\theta) = p(1-\theta) - \theta(1-\theta)^2.$$

It is convenient to write

$$f(\theta) = -\partial/\partial\theta U(\theta),$$

with "potential"

$$U(\theta) = \tfrac{1}{2}p(1-\theta)^2 - \tfrac{1}{3}(1-\theta)^3 + \tfrac{1}{4}(1-\theta)^4. \tag{A2}$$

The stable steady states correspond to the minima of U—i.e., $\theta=\theta_{\text{absorb}}=1$ for all p (the absorbing state) and $\theta=\theta_{\text{active}}(p)=\frac{1}{2}-\frac{1}{2}(1-4p)^{1/2}$ for $p<p_s(\text{mf})=\frac{1}{4}$ (the stable active state). These are separated by an unstable steady state with $\theta=\theta_{\text{unstable}}(p)=\frac{1}{2}+\frac{1}{2}(1-4p)^{1/2}$ for $p<p_s(\text{mf})=\frac{1}{4}$, corresponding to a local maximum of U.

To analyze propagation of planar interfaces with velocity V between active and absorbing states, one considers solutions of the form $\theta=\theta(x-Vt)$ [47,48]. Substitution into Eq. (A1) yields

$$D\theta'' = -\partial/\partial\theta[-U(\theta)] - V\theta', \tag{A3}$$

where the prime denotes derivative with respect to the single variable. This Newton-type equation describes the motion of a pseudoparticle with position θ subject to a two-hill potential $-U(\theta)$ and subject to a drag force with drag coefficient V. The physical interface corresponds to motion from one hill to the other with (almost) vanishing initial and final velocities. Equistability corresponds to the case $V=0$, which by conservation of energy requires that the two hills have equal height. A simple calculation shows that this corresponds to $p=p_{\text{eq}}(\text{mf})=\frac{2}{9}\approx 0.222$ (mean-field) [1,48]. This result also follows as a special case of the analysis of the general mean-field Schloegl model of the second kind [17], where it is shown that

$$V \propto (\theta_{\text{absorb}} + \theta_{\text{active}} - 2\theta_{\text{unstable}}). \tag{A4}$$

This expression also shows that V has a finite value, V_s, say, at the spinodal $p=p_s(\text{mf})=\frac{1}{4}$ and that $V-V_s \sim (1-4p)^{1/2}$, as $p \to p_s(\text{mf})$. The nonlinear behavior as p approaches p_s is reminiscent of the behavior shown in our simulation results for $V(S,p)$ for the QCP in Fig. 10.

APPENDIX B: MODIFICATIONS AND GENERALIZATIONS OF THE QCP

We consider the following modifications or generalizations of the standard QCP.

(i) Addition to the QCP of a separate random desorption pathway associated with a "small" desorption rate $d \geqslant 0$ [19]. Making an analogy with the conventional equilibrium Ising model, d corresponds to a temperaturelike variable, with $d=0$ recovering the standard QCP. This generalized model removes the special feature of standard QCP rules which prohibits growth of isolated empty droplets and which prohibits the shrinkage of vertical strip of the absorbing state. However, we find that generic two-phase coexistence persist in this generalized model extending to a range of $d>0$. PC terminates at an Ising-type critical point $d=d_c$ [19]. A detailed analysis of this generalized model will be provided elsewhere. This observation supports the claim made above that the presence of an absorbing state in the QCP should not be regarded as producing PC. It should also be noted that this generalized model constitutes just one way of perturbing the desorption rates in the QCP, and we find that various other perturbations will also preserve generic two-phase coexistence.

(ii) An adsorption-desorption version of the QCP on a triangular lattice (with coordination number 6): adsorption

occurs randomly at rate p, and cooperative desorption of particles occurs at rate $k/4$ where $k=0$, 1, 2, 3, 4, or 6 denotes the number of adjacent pairs of NN empty sites. Interestingly, the mean-field kinetics remains unchanged from the case of the square lattice in contrast to the conversion of the type of transition. CC simulation studies reveal a continuous transition to the absorbing state occurs at $p \approx 0.177$. The simulated steady-state coverage in the active state actually follows the mean-field value from Appendix A more closely and for higher p than for the QCP on the square lattice. This feature is presumably a consequence of the higher coordination number for the triangular lattice. However, eventually the steady-state coverage for the QCP on the triangular lattice departs strongly from MF behavior in the vicinity of the continuous transition.

(iii) Relaxation of the constraint on desorption in the QCP so that now any particle with two or more empty neighbors can desorb. Choosing the desorption rate to always equal unity, this process corresponds to the threshold contact process for $M=2$ [20]. A previous study proved the existence of a phase transition, but did not determine its nature [20]. Our own simulation study reveals the existence of a discontinuous transition at $p_{eq}^{*} \approx 0.36$ (starting from an empty lattice) which should be compared with $p_{eq}^{*} \approx 0.0944$ for the QCP. Generic two-phase coexistence also occurs. The substantial increase in adsorption rate p_{eq}^{*} from its value for the standard QCP is readily understood since the effective desorption rate is also significantly higher than in the standard QCP. An additional perspective comes from applying a mean field analysis wherein

$$d\theta/dt = p(1-\theta) - \theta(1-\theta)^2(1+2\theta+3\theta^2), \qquad \text{(B1)}$$

for the $M=2$ threshold contact process.

From Eq. (B1), one finds a spinodal pressure $p_s \approx 0.678$ for this process versus $p_s \approx 0.25$ for the QCP, so the increase in the mean field p_s mimics the increase in p_{eq}^{*}. Some other features of this threshold contact process should be noted. Like the QCP, one still has the special feature that vertical (or horizontal) strips of the absorbing phase cannot be eroded and that empty patches embedded in the absorbing state cannot grow outside of a rectangular region inscribing them. The irreversible erosion of planar interfaces for $p=0$ is identical to that in the QCP. Relaxation kinetics for $p=0$ or $p=0+$ is described by the standard BP model.

[1] R. Durrett, SIAM Rev. **41**, 677 (1999).
[2] J. Marro and R. Dickman, *Nonequilibrium Phase Transitions in Lattice Models* (Cambridge University Press, Cambridge, England, 1999).
[3] H. Hinrichsen, Adv. Phys. **49**, 815 (2000).
[4] G. Odor, Rev. Mod. Phys. **76**, 663 (2004).
[5] R. M. Ziff, E. Gulari, and Y. Barshad, Phys. Rev. Lett. **56**, 2553 (1986).
[6] J. W. Evans and M. S. Miesch, Phys. Rev. Lett. **66**, 833 (1991).
[7] J. W. Evans and T. R. Ray, Phys. Rev. E **50**, 4302 (1994).
[8] R. H. Goodman, D. S. Graff, L. M. Sander, P. Leroux-Hugon, and E. Clément, Phys. Rev. E **52**, 5904 (1995).
[9] R. A. Monetti and E. V. Albano, J. Phys. A **34**, 1103 (2001).
[10] E. Loscar and E. V. Albano, Rep. Prog. Phys. **66**, 1343 (2003).
[11] E. Machado, G. M. Buendia, and P. A. Rikvold, Phys. Rev. E **71**, 031603 (2005).
[12] Da-Jiang Liu, Xiaofang Guo, D. Unruh, and J. W. Evans (unpublished).
[13] R. Bidaux, N. Boccara, and H. Chaté, Phys. Rev. A **39**, 3094 (1989).
[14] R. Dickman and T. Tomé, Phys. Rev. A **44**, 4833 (1991).
[15] G. A. Cardozo and J. F. Fontanari, Eur. Phys. J. B **51**, 555 (2006).
[16] F. Schloegl, Z. Phys. **253**, 147 (1972).
[17] A. L. Mikhailov, *Foundations of Synergetics I* (Springer-Verlag, Berlin, 1990).
[18] P. Grassberger, Z. Phys. B: Condens. Matter **47**, 365 (1982).
[19] D.-J. Liu, Xiaofang Guo, and J. W. Evans, Phys. Rev. Lett. **98**, 050601 (2007).
[20] S. J. Hanjini, J. Theor. Probab. **10**, 737 (1997).
[21] M. A. Munoz, F. de los Santos, and M. M. T. da Gama, Eur. Phys. J. B **43**, 73 (2005).
[22] A. L. Toom, in *Multicomponent Random Systems*, edited by R. L. Dobrushin and Y. G. Sinai (Marcel Dekker, New York, 1980).
[23] C. H. Bennett and G. Grinstein, Phys. Rev. Lett. **55**, 657 (1985).
[24] G. Grinstein, IBM J. Res. Dev. **48**, 5 (2004).
[25] Y. He, C. Jayaprakash, and G. Grinstein, Phys. Rev. A **42**, 3348 (1990).
[26] M. Bramson and L. Gray, in *Random Walks, Brownian Motion, and Interacting Brownian Motion*, edited by R. Durett and H. Keston (Birkhauser, Boston, 1991).
[27] R. M. Ziff and B. J. Brosilow, Phys. Rev. A **46**, 4630 (1992).
[28] J. W. Evans, D.-J. Liu, and M. Tammaro, Chaos **12**, 131 (2002).
[29] D.-J. Liu and J. W. Evans, J. Phys.: Condens. Matter **19**, 065129 (2007).
[30] R. H. Schonmann and S. B. Shlosman, Commun. Math. Phys. **194**, 389 (1998).
[31] S. Shlosman, Physica A **263**, 180 (1999).
[32] Xiaofang Guo, J. W. Evans, and Da-Jiang Liu, Physica A (to be published).
[33] M. Avrami, J. Chem. Phys. **7**, 1103 (1939); **8**, 212 (1940); **9**, 177 (1941).
[34] J. W. Evans, Rev. Mod. Phys. **65**, 1296 (1993).
[35] D. E. Sanders and J. W. Evans, Phys. Rev. A **38**, 4186 (1988).
[36] J. Adler and A. Aharony, J. Phys. A **21**, 1387 (1988).
[37] J. Adler, D. Stauffer, and A. Aharony, J. Phys. A **22**, L297 (1989).
[38] M. Aizenman and J. L. Lebowitz, J. Phys. A **21**, 3801 (1988).
[39] An exact analysis of standard BP indicates that there must exist a crossover in γ for larger L. to a precise asymptotic value of $\gamma=\pi^2/18 \approx 0.55$. See A. Holroyd, Probab. Theory Relat. Fields **125**, 195 (2003).

[40] J. W. Evans and H. C. Kang, J. Math. Phys. **32**, 2918 (1991).
[41] P. Meakin, P. Ramanlal, L. M. Sander, and R. C. Ball, Phys. Rev. A **34**, 5091 (1986).
[42] J. Krug and H. Spohn, Europhys. Lett. **8**, 219 (1989).
[43] H. Hinrichsen, R. Livi, D. Mukamel, and A. Politi, Phys. Rev. E **61**, R1032 (2000).
[44] C. H. Bennett, G. Grinstein, Y. He, C. Jayaprakash, and D. Mukamel, Phys. Rev. A **41**, 1932 (1990).
[45] J. D. Gunton and M. Droz, *Introduction to the Theory of Metastable and Unstable States, Springer Lecture Notes in Physics*, Vol. 183 (Springer, Berlin, 1983).
[46] R. Kutner, Phys. Lett. **81A**, 239 (1981).
[47] P. C. Fife and J. B. McLeod, Arch. Ration. Mech. Anal. **65**, 335 (1977).
[48] C. Noble, Ann. Probab. **20**, 724 (1992).